
Article:
Payne, T., Williams, A., Worfolk, T. et al. (1 more author) (2016) Numerical investigation into the influence of cubicle positioning in large-scale explosive arena trials. International Journal of Protective Structures, 7 (4). pp. 547-560. ISSN 2041-4196

https://doi.org/10.1177/2041419616676438

Title: Numerical investigation into the influence of cubicle positioning in large-scale explosive arena trials

Authors: Thomas Payne[1*], Andrew Williams[1], Thomas Worfolk[1], Samuel Rigby[2]

Abstract

In arena blast testing, a common and economical practice employed is to distribute several targets radially around a central charge. However, if these targets are positioned too proximally, reflections and diffractions of blast waves off neighbouring cubicles can affect the nature of expected blast loading.

Computational fluid dynamics software has been used through an extensive series of simulations to identify the levels of interference in incident pressure-time histories with and without an obstructing target present. The data were post-processed to identify the Cartesian co-ordinates in which different levels of interference in peak incident overpressure (Ps^+) and incident positive phase impulse (Is^+) were achieved.

The results indicated that, in all cases, there was a greater interference in Ps^+ than Is^+ values directly proximal to the target but, at greater separations, significant differences in Is^+ existed where Ps^+ had returned to free-field equivalent magnitudes. When compared with established 'rules of thumb' for cubicle placement, for targets at different stand-off ranges, an angle of 45° to the rear cubicle still holds some practical relevance. However, for targets positioned at the same stand-off range, a separation distance of two cubicle widths is generally too conservative and, in many cases, more cubicles can be positioned around the charge.

A bespoke recommendation table has been presented for targets at stand-off ranges between 15 and 50 m to allow users to identify the minimum distance from a target at which obstructed-field Ps^+ and Is^+ values differ negligibly from free-field equivalents.

Keywords

Blast, computational fluid dynamics (CFD), arena testing, cubicle placement, clearing

Word Count: 243 (Abstract); 3,809 (Main Body)

Abbreviations:

CFD computational fluid dynamics
Ps^+ peak incident overpressure
Is^+ incident positive phase impulse
Pr^+ peak positive reflected pressure
Ir^+ reflected positive phase impulse
TNT_e TNT equivalence

[1] Home Office – Centre for Applied Science and Technology, Langhurst House, RH12 4WX.
[2] Department of Civil and Structural Engineering, University of Sheffield, Mappin Street, Sheffield S1 3JD.

1. Introduction

In large-scale arena blast trials, a common and economical practice often undertaken is to distribute several targets radially around a central charge, and, assuming a spherical blast wave, infer identical loading for targets at the same stand-off. In many cases, targets will also be positioned at different stand-off ranges to elicit variations in loading phenomena. Issues may arise from the proximity of neighbouring targets, which, if too close, can result in unexpected blast-wave structure interactions.

When a blast wave hits a target of finite size it reflects from it and diffracts around it, modifying the pressure-time histories of nearby waves. Reflections can result in an amplification effect through a superposition with the incident blast wave, whilst diffractions can result in a shielding (or shadowing) effect with decreased blast wave intensity in the region behind the structure (Remennikov and Rose, 2005; Needham, 2009). This has been shown schematically in Figure 1.

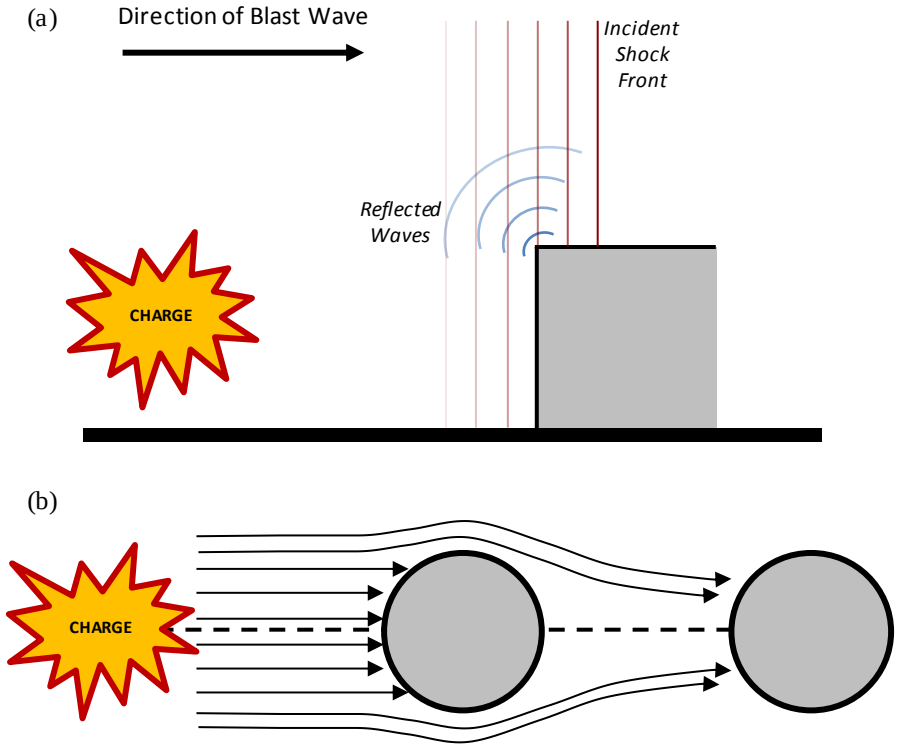

Figure 1 – Schematic showing formation of: (a) an amplification effect and (b) a shielding effect.

Previous research investigating blast-wave structure interactions has focused largely on the local 'clearing' effects experienced by structures of finite size when exposed to a blast wave (Rickman and Murrell, 2007; Shi et al., 2007; Ballantyne et al., 2009; Qasrawi et al., 2015). Recent studies have led to new perspectives on the mechanisms for the clearing effect and proposed methods to calculate their extent (Rigby et al., 2014a).

With regards to the global effects of these interactions, in terms of blast wave interference, a growing body of recent research has been conducted investigating loading on structures in urban streetscape environments. Early work on such effects was conducted by Smith and Rose (2000) who investigated the features of urban streetscape environments that amplify the magnitude of resultant blast wave parameters using experimental study and computational fluid dynamics (CFD) software. Remennikov and Rose (2005) subsequently conducted a detailed series of numerical simulations using Air3D CFD

software to investigate the extent of shadowing and amplification effects from adjacent buildings in an urban terrain. The authors quantified changes in the magnitude of pressure and impulse in a range of scenarios. In recent years, a significant focus has been placed upon internal explosions and channelling effects introduced in different building geometries. Codina et al. (2013) conducted an extensive series of parametric numerical simulations using the ANSYS AUTODYN hydrocode. They studied the mechanisms for channelling behaviour in confined and unconfined geometries, and quantified the effects based on a range of street width and charge mass parameters.

However, there remains a paucity of research studying the specific interferences introduced due to the proximity of neighbouring structures in arena blast trials. In such testing, two 'rules of thumb' are typically used as a guideline for engineers in the field, indicating separations at which blast wave interferences are assumed to be no longer significant and equivalent of free-field conditions.

- For two cubicle targets at the same stand-off range: separation of two cubicle widths.
- For two cubicle targets at different stand-off ranges: a minimum angle of 45° between targets measured from the detonation point.

Pressure and impulse are widely acknowledged to be the two key contributory factors relating to blast load damage on structures. Although negative phase has been shown to be influential in blast damage, particularly in more frangible structures (Rigby et al., 2014b), the present analysis focuses on rigid targets and these effects have been neglected. Examination of the interference effects to these positive phase loading phenomena from rigid target obstructions can enable more informed cubicle placement in arena blast trials. Such information could also be used to verify the veracity of existing rules of thumb and potentially permit a greater amount of cubicles to be positioned around a charge, thus reducing costs.

This study aims to use conventional numerical modelling techniques to examine the influence of cubicle positioning in large-scale arena blast trials and present a series of recommendations for placement in a format that can easily be used by engineers in the field.

2. Methodology

2.1. Modelling software

Computational fluid dynamics (CFD) software package Air3D (Cranfield University, UK) was used for all simulations in this study (Rose, 2006) as the software provided a verified level of blast wave fidelity and phenomenology whilst possessing a relatively low computational expenditure.

There are a number of assumptions, however, associated with the use of this software that make the computations more efficient. In brief, these are:

- the ground surface and targets are considered perfectly rigid;
- the impact of thermal shocking and detonation products are ignored;
- air and other gaseous products are treated as ideal; and
- the blast wave is assumed to be spherical.

2.2. Modelling approach

To determine the influence of arena test cubicles on nearby blast waves, a series of paired simulations were run: one free-field and the other with a single obstructing cubicle target present. The differences in incident overpressure-time histories were then examined between free-field and obstructed-field simulations to identify the degree of interference in peak incident overpressure (Ps^+) and incident positive phase impulse (Is^+) from each test configuration.

In each simulation, the target cubicle was fixed at a range of between 15 and 50 m in 5 m intervals. The cubicle was given dimensions of 3.50 m × 3.95 m × 3.00 m (width × height × depth), representative of a typical wall target, in all simulations. Arrays of pressure gauges were radially distributed in an arc from the explosive source. Each array contained a total of 400 gauges evenly distributed over the region of interest at a height of 2.00 m (approximately half the cubicle height). The gauge arcs were positioned in 5 m stand-off intervals from the target (i.e. a 35 m stand-off target would have gauges on arcs at 35 m, 40 m, 45 m and 50 m stand-off ranges). For all simulations, a 100 kg TNT equivalence (TNT_e) charge (Air3D default charge parameters) was used. An example 2D schematic of the test configuration has been shown in Figure 2.

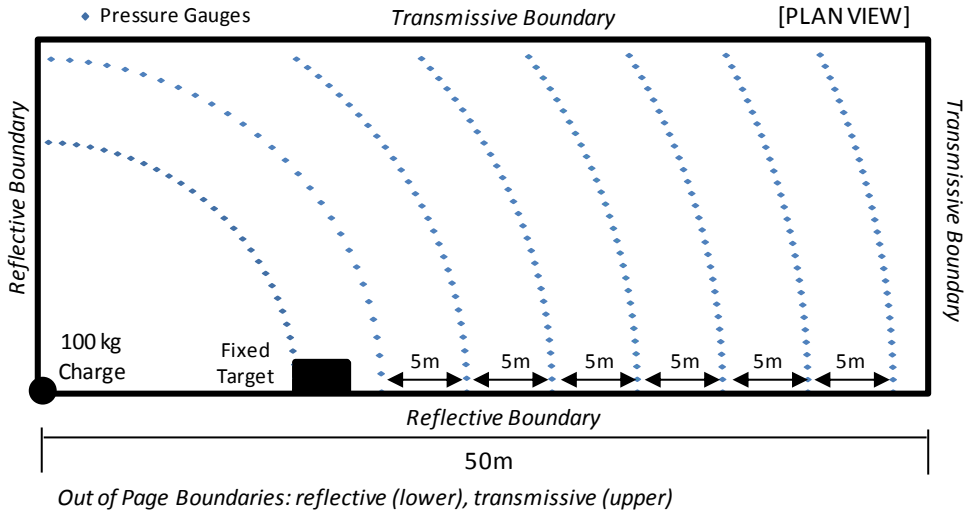

Figure 2 – Schematic of simulation test configuration.

2.3. Model development

In Air3D, explosive simulations are treated in a multi-stage process through 1D, 2D and 3D domains. In the 1D domain, the simulation is performed to model the formation of the wave up to the nearest surface. As it reaches the ground, it ceases to be spherically symmetric and the solution is remapped into 2D with a reflective ground surface and an axisymmetric simulation is run that models blast wave formation and propagation up to the point where it interacts with the first target structure. Once it reaches an obstacle, it is no longer axisymmetric and the solution is remapped to a 3D domain where the interaction between the blast wave and the structural target is simulated.

In the 2D model, a 14.9 m × 14.9 m domain was used, whilst in 3D domain boundaries in x, y and z were altered based on the measurement region of interest both to reduce computational costs and limit boundary effects. Quarter symmetry was applied to the model with reflective boundaries in the lower x, y and z planes as shown in Figure 2.

Mesh refinements were conducted in all domains to ensure that blast phenomena were adequately represented at minimal computational cost. The Air3D version 9.0 users' guide (Rose, 2006) states that *"problems should be set up initially using a discretisation that allows an accurate description of* the problem geometry and captures all major aspects of the flow-field: correct number and duration *of shock waves"*.

A series of iterative mesh refinement simulations informed the use of 1 mm and 20 mm cell sizes for 1D and 2D simulations respectively. 3D mesh refinement simulations were compared with CONWEP hemispherical burst parameters to provide a measure of the absolute accuracy of predictions (Figure 3).

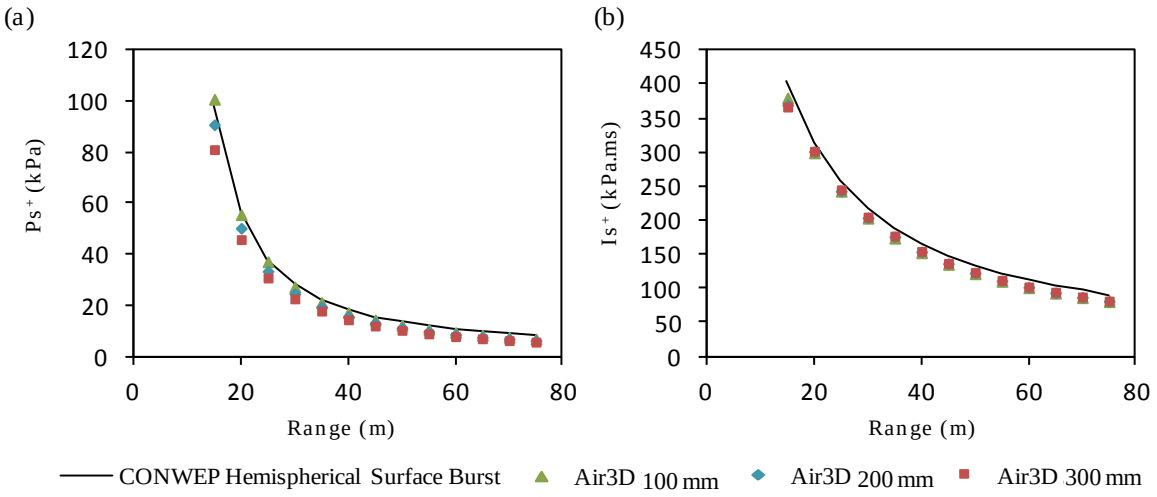

Figure 3 – Comparison of Ps^+ and Is^+ of different cell size simulations against CONWEP hemispherical burst predictions.

A 3D cell size of 100 mm was selected due to its accuracy relative to computational costs. The 100 mm cell size simulations provided solutions with maximum differences of +1.78% and -5.73% in Ps^+ and Is^+ respectively from CONWEP hemispherical burst predictions. Only minor improvements of -0.80% and -0.13% were recorded in Ps^+ and Is^+ respectively with a finer 80 mm cell size despite a +1,930% difference in computational time.

To validate the reflection and diffraction effects generated by Air3D, peak positive reflected pressure (Pr^+) and peak reflected positive phase impulse (Ir^+) values from simulations were compared with experimental test data from blast trials conducted at the University of Sheffield (Tyas et al., 2011). The experiments were designed to investigate blast wave clearing effects on rigid targets positioned at ranges of 4 – 10 m using 250 g C4 hemispherical explosive charges. The rigid targets had frontal dimensions of 675 mm × 710 mm with two pressure gauges, one in the centre of the face and the other 25% of the target height above it; the central gauge has been used for comparison in this study. Figure 4 shows a comparison between experimental test data and Air3D predictions with the magnitudes of Pr^+ and Ir^+ compared in Table 1 with the percentage difference between Air3D and the mean experimental data also shown.

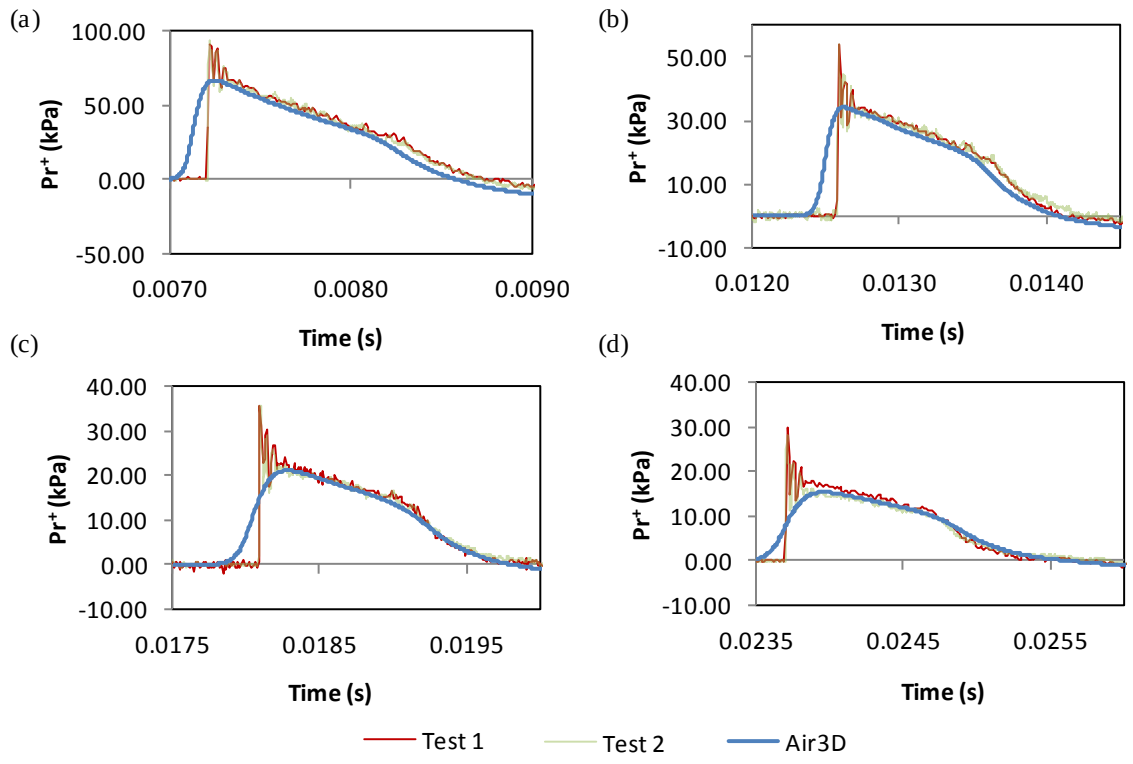

Figure 4 – Comparison between Air3D predictions and experimental test data (Tyas et al., 2011) for targets at: (a) 4 m; (b) 6 m; (c) 8 m; and (d) 10 m ranges.

Table 1 – Comparison of Pr^+ and Ir^+ values between experimental study (Tyas et al., 2011) and Air3D predictions.

	Pr^+ (kPa)					Ir^+ (kPa.ms)				
	T1	T2	Mean	Air3D	% Difference	T1	T2	Mean	Air3D	% Difference
4 m	68.2	69.9	69.1	67.0	-3.04	56.0	57.2	56.6	55.2	-2.47
6 m	38.1	36.9	37.5	34.2	-8.80	32.7	32.4	32.6	32.0	-1.84
8 m	23.8	22.9	23.4	21.2	-9.40	22.9	22.8	22.9	22.4	-2.18
10 m	18.1	16.8	17.5	15.4	-12.0	17.1	17.8	17.5	17.0	-2.86

The data indicate that AirD provides an acceptable estimate of experimental trials data with representative pressure-time history responses and maximal differences in Pr^+ and Ir^+ of -12.0% and -2.86% respectively. Impulse values exhibit greater differences as they are affected by numerical energy losses and are generally lower in computational models than experimentally recorded values. However, diffraction effects (in terms of arrival time and magnitude of the clearing wave) are recorded accurately.

2.4. Post-processing

Given the significant quantities of data produced by the arrays of pressure gauges, MATLAB® (Mathworks Ltd., MA, USA) was selected as the post-processing tool due to its robust and efficient processing capabilities.

In each simulation, the pressure-time histories extracted from Air3D were imported into MATLAB® and processed to determine Ps^+ and Is^+ values. The array of Ps^+ and Is^+ values from the free-field simulations were then processed alongside the corresponding values from the obstructed-field simulations to calculate the percentage difference (interference) at each gauge. Given an array of percentage difference values for Ps^+ and Is^+, a threshold value was applied and the corresponding Cartesian co-ordinate location was identified.

For instances where the fixed target and measurement location was at the same stand-off range from the charge, the straight line distance between the edge of the fixed target and the threshold co-ordinate was determined using simple Pythagoras (Figure 5a). For instances where the fixed target was at a different range to the measurement location, the most practically useful measure of separation was determined to be the straight line separation from the fixed target at the same range. To achieve this, the equation of the line from the threshold point to the origin was calculated, which was used to determine the intersection with the fixed target gauge arc (Figure 5b). This point was then, in turn, used to calculate the straight line distance to the fixed target edge.

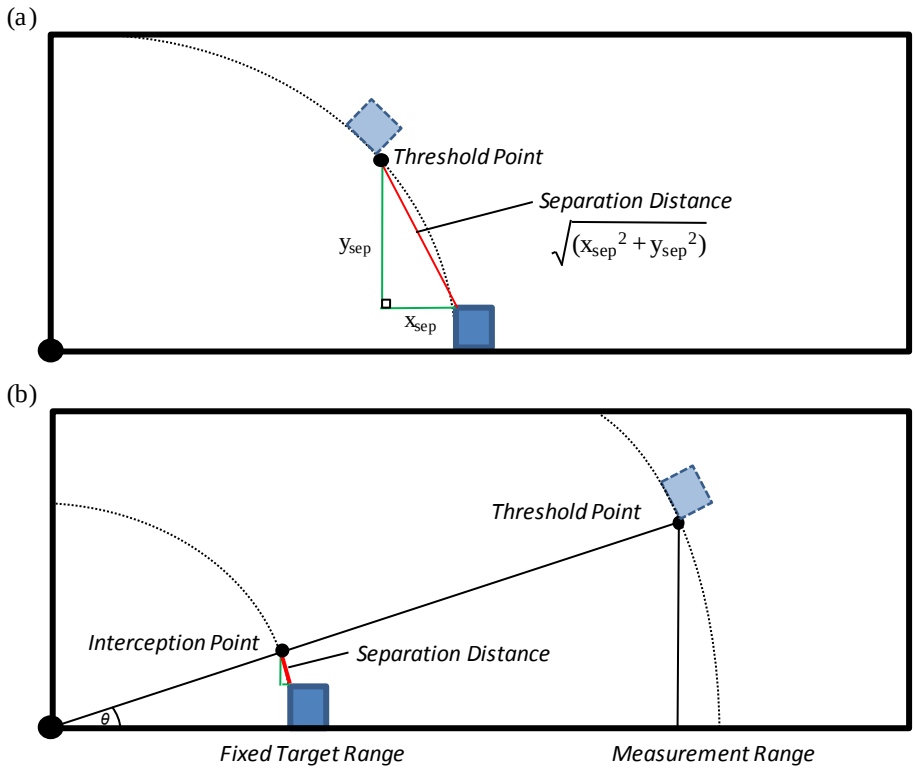

Figure 5 – Schematic showing the calculations performed to determine minimum separation distances at different interference thresholds when the fixed target and measurement positions are at: (a) the same stand-off range; and (b) different stand-off ranges.

3. Results

3.1. General trends

The visualisations in Figure 6 show, in plan view, an example of peak incident overpressure (Ps^+) and incident positive phase impulse (Is^+) interference fields around a fixed target cubicle positioned at a 15 m stand-off range recorded at approximately 2 m above ground level. It is evident that there are differences in the magnitudes of effects of Ps^+ and Is^+ and the regions affected by the target. It is also clear that there are significantly greater differences in Ps^+ than Is^+ in the immediate proximity to the fixed target.

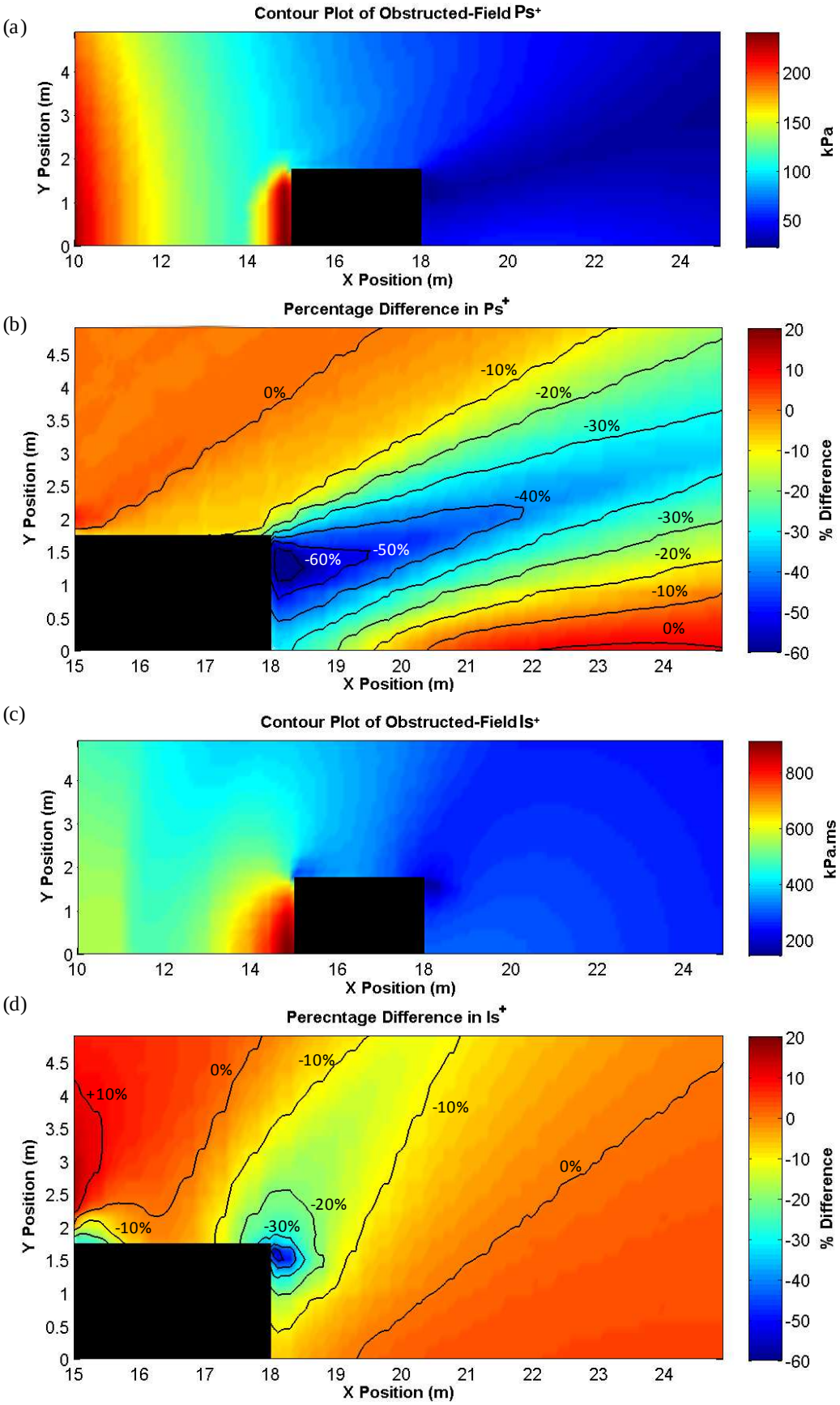

Figure 6 – Visualisations of interference by a fixed target obstacle at 15 m. Contour plots show examples of: (a) obstructed-field Ps^+; (b) percentage differences in Ps^+; (c) obstructed-field Is^+; and (d) percentage difference in Is^+.

Figure 7 shows the radial distances from the fixed target to the position of maximum interference and limit of interference (free-field equivalent position) for Ps^+ and Is^+. In all cases, the maximum interference and the limit of interference in Ps^+ occurs at much closer proximity to the target than Is^+.

Assuming the relationship to be linear, the critical angles for maximum interference and limit of interference were 21.7° and 35.7° in Ps^+ respectively, and, 39.7° and 44.6° in Is^+ respectively. From these values, the angle for 'limit of interference' in Is^+ appears to correspond well with the 45° recommended in established rules of thumb.

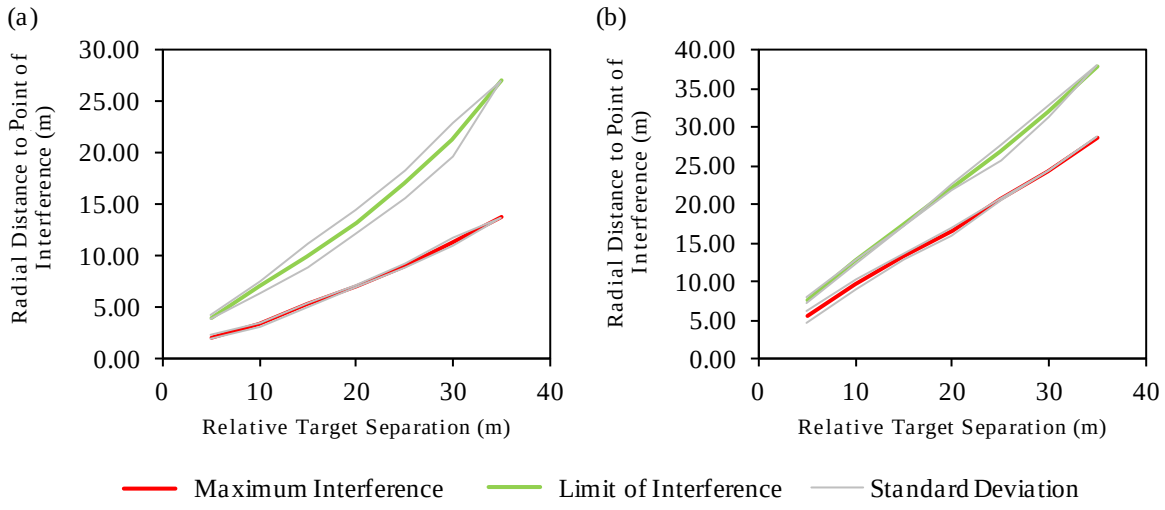

Figure 7 – Graphs showing the levels of interference introduced by fixed target obstacles at different relative target separations for: (a) Ps^+; and (b) Is^+.

3.2. Measurements at the same range as the fixed target

Figure 8 shows a representative example of the levels of interferences in Ps^+ and Is^+ introduced by a fixed target obstruction when measuring on an arc at the same stand-off range. The interferences introduced at the same range are amplifications of the Ps^+ and Is^+ magnitudes close to the target. It is also evident that, at the same range, there are more significant differences in Ps^+ than Is^+ in the immediate proximity though values return to free-field equivalent at a much closer separation. In the example shown, maximal differences of +179% in Ps^+ exist immediately proximal to the target, whilst reduced differences of +144% are shown in Is^+ in the same spatial position. However, 4 m from the fixed target, Ps^+ values returned to free-field equivalent magnitudes (~0% interference) whilst Is^+ differences of 10.7% were exhibited.

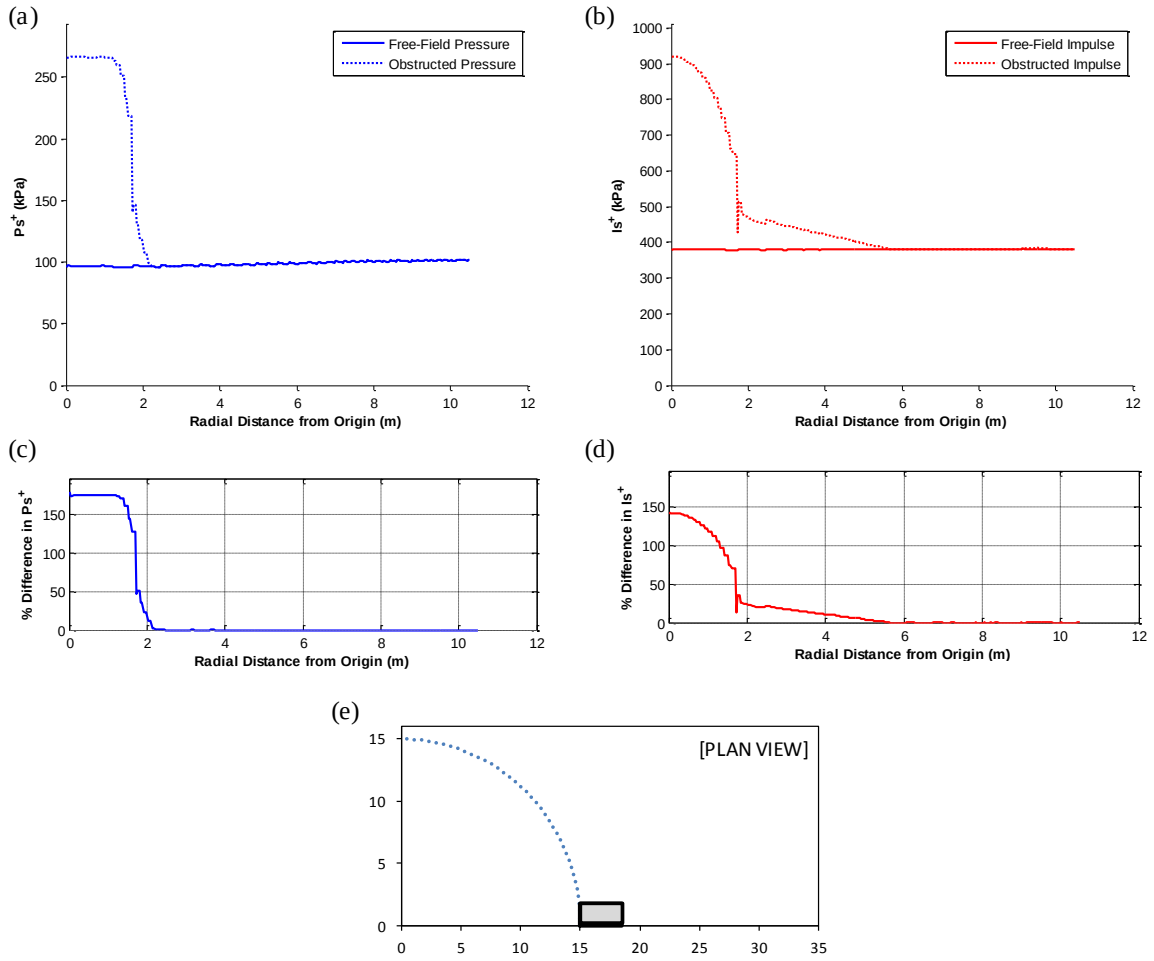

Figure 8 – A comparison between measurements from free-field and obstructed-field gauges for a 15 m fixed target with a 15 m measurement range. Graphs showing: (a) free-field and obstructed-field Ps^+; (b) free-field and obstructed-field Is^+; (c) percentage differences in Ps^+; (d) percentage differences in Is^+; and (e) example test configuration.

3.3. Measurements at greater stand-off distances than the fixed target

Figure 9 shows a representative example of the effects experienced when measurements were taken at greater stand-off ranges to the fixed target. There is evidently a shadowing effect elicited with decreased magnitudes of Ps^+ and Is^+ at the measurement range behind the target. Similar to the same range measurements, greater differences in Ps^+ were exhibited close to the target but values return to free-field equivalent magnitudes relatively close to the target, whilst more significant differences were elicited in Is^+ at much greater separations from the target. In the given example, differences in Ps^+ reached a maximum of -47.7% at a distance 1.69 m from the target, whilst maximal differences in Is^+ of -13.9% are experienced 4.08 m from the target. Free-field equivalency is achieved in Ps^+ and Is^+ at separations of 4.55 m and 6.71 m respectively.

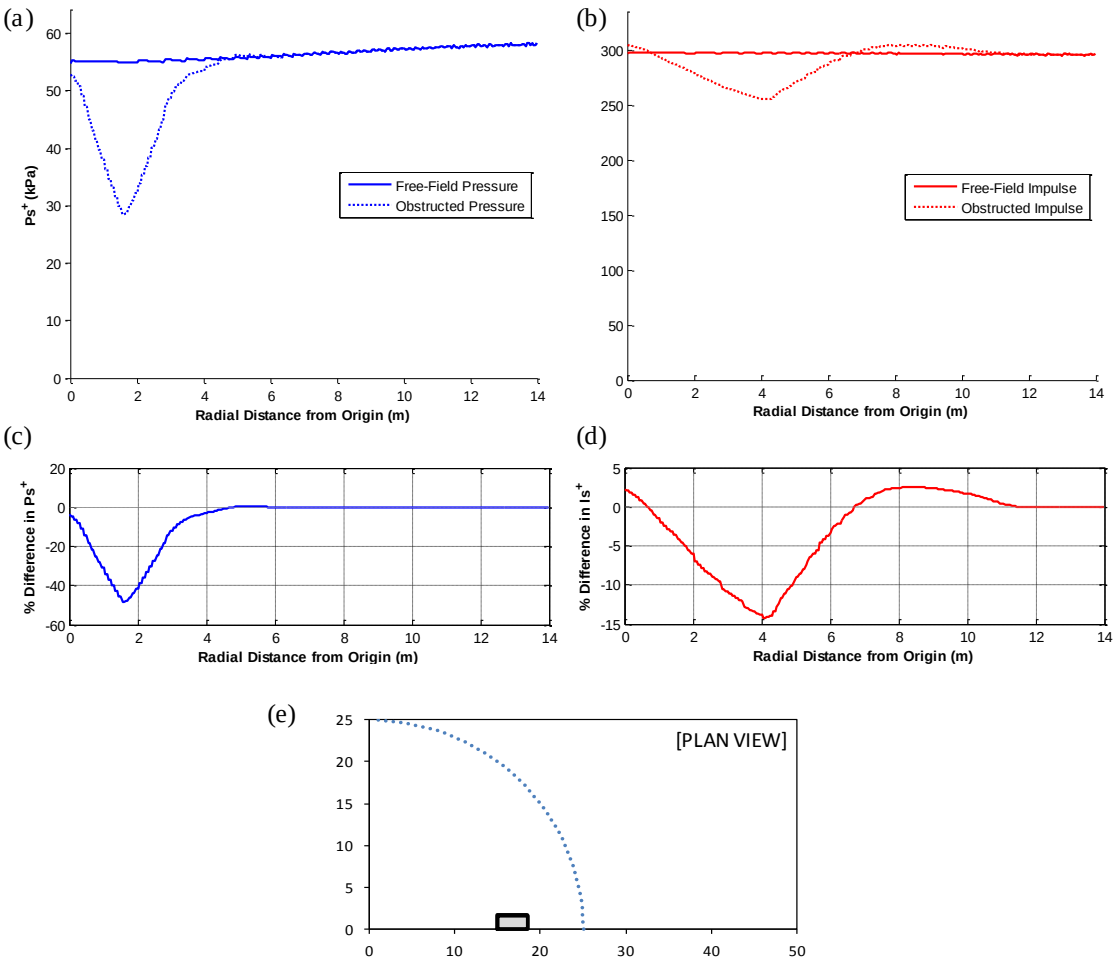

Figure 9 – A comparison between measurements from free-field and obstructed-field gauges for a 15 m fixed target with a 20 m measurement range. Graphs showing: (a) free-field and obstructed-field Ps^+; (b) free-field and obstructed-field Is^+; (c) percentage differences in Ps^+; (d) percentage differences in Is^+; and (e) example test configuration.

In Figure 8 and Figure 9, there is a clear deviation in the magnitudes of free-field Ps^+ and Is^+ exhibited with an appreciable drift further from the origin. This artefact is better illustrated in Figure 10 and can potentially be attributed to positional rounding errors from gauges closer to the 45° position on the arc. A maximal difference in Ps^+ of 5.88% was calculated in the 20 m stand-off range arc. However, it

is not anticipated that these variances will be significant as, in all cases, relative differences have been examined.

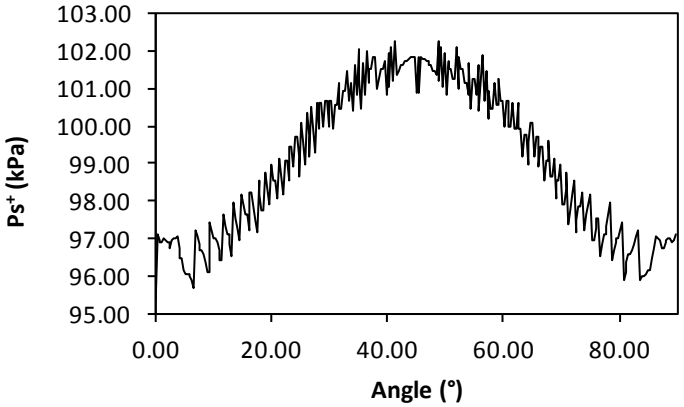

Figure 10 – Graph showing parabolic Ps^+ distribution from gauges on a 20 m radial arc.

3.4. Recommended separation distances

As greater separation distances were required to elicit free-field equivalent Is^+ values than Ps^+, impulse predictions have been used to derive a series of recommended separation distances for cubicle targets in blast testing arenas. It is to be noted that the values in this table represent the separation distances required at the same range as the fixed target and, where necessary, should be used to infer target position at greater stand-off distances via the method shown in Figure 5b as the angle of the 'limit of interference' has been shown to be effectively constant with increasing distance from the explosive origin as in Figure 7.

Table 2 presents the recommended separation distances to achieve free-field equivalent Ps^+ and Is^+ values for targets at a stand-off range between 15 and 50 m. The terms 'fixed target location' and 'variable target location' in this table pertain to the method by which cubicles should be positioned. The fixed target is considered stationary with the variable target positioned relative to it.

Table 2 – Recommended clear separation distances to achieve representative (0% interference) free-field Ps^+ and Is^+ values for fixed and variable targets at different stand-off ranges.

Fixed Target Location \ Variable Target Location	15 m	20 m	25 m	30 m	35 m	40 m	45 m	50 m
15 m	3.88	3.30	5.55	6.88	7.96	8.70	9.21	9.64
20 m		4.58	4.03	6.49	8.08	9.50	10.1	10.7
25 m			5.03	4.51	7.18	8.97	10.5	10.9
30 m				5.26	4.72	7.87	9.87	11.2
35 m					5.58	5.42	8.32	10.3
40 m						5.99	5.48	12.1
45 m							6.87	5.83
50 m								6.92

4. Discussion

4.1. Overview of recommendations

The present study provided a series of recommendations for cubicle positioning in arena blast trials through the determination of the differences in free-field pressure-time histories, with and without an obstructing target present, using numerical modelling techniques. In all conditions, there was a greater interference to peak incident overpressure (Ps^+) values than to incident positive phase impulse (Is^+) values in the region immediately proximal to the fixed target. However, Ps^+ values returned to free-field equivalents relatively close to the target, whilst Is^+ values remained significant at greater distances. Consequently, Is^+ interferences governed separation distance recommendations.

To examine the appropriateness of existing rules of thumb used by engineers in the field, a direct comparison has been made with the new recommendations. In established rules of thumb, for targets at the same range, assuming a wall target of 3.50 m width, a practical recommendation of 7 m is given (two cubicle widths). The recommendations from the present study vary between 3.88 m and 6.92 m based on target range. This suggests that the rule of thumb is of a similar magnitude to predictions in far-field conditions, though is conservative for targets in the near field where a smaller separation could be applied and more targets could potentially be distributed around the charge. The minimum separation angle of 45° established corresponds very well with the angle for the limit of Is^+ interference of 44.6°. However, it should be noted that the angles derived in this study have been based on an average angle taken from many simulations with different fixed target ranges and measurement positions (same relative separation). Therefore, it is likely that there will be variations based on individual test configurations. Although 45° acts as a reasonable estimate, there will be many situations where this rule of thumb will not be appropriate and the table recommendation distances should supersede the established rules of thumb.

4.2. Sensitivity analysis

A sensitivity analysis was conducted to investigate differences in separation distance predictions when the target size was varied between the minimum and maximum dimensions commonly used in cubicles for arena blast testing. In each simulation, a single dimension was altered and the differences from the standard cubicle size predictions were recorded.

For this analysis, the fixed targets were positioned at a distance of 15 m from the charge with measurements at 15 m and 25 m ranges. Differences in blast parameters from the test cubicle recommendations have been shown in Table 3.

Table 3 – Percentage differences in Ps^+ and Is^+ when dimensions of the standard wall cubicle target were individually altered within representative pre-defined limits.

		x_{depth+}	x_{depth-}	x_{width+}	x_{width-}	$x_{height+}$	$x_{height-}$
15 m Fixed Target – 15 m Measurement Position	Ps^+	0.00	0.00	-146.26	53.63	0.00	0.00
	Is^+	-3.79	3.58	-100.62	30.38	-10.07	7.07
15 m Fixed Target – 25 m Measurement Position	Ps^+	24.69	-32.47	-33.51	22.08	-2.79	0.97
	Is^+	14.93	-18.04	-9.67	7.26	-4.96	0.50

When the fixed target and measurement position were at the same range, the sensitivity analysis showed that variations in target depth and height had no effect on Ps^+ predictions. Similarly,

differences in Is^+ in each of these variables were small (maximum -10.07% difference). Changes to the fixed target width, however, resulted in significant differences to both Ps^+ and Is^+ recommendations.

When the fixed target and measurement position were at different ranges, smaller differences in predictions were generally observed. There were only very minor differences in predictions when the height of the fixed target was changed (maximum -4.96% difference). Increases to the depth of the target and reductions to the width of the target resulted in the need for increased separation distances. In both cases, greater differences were recorded in Ps^+ than in Is^+.

In conclusion, the recommendations given should remain unchanged when the target height is altered but cannot accurately be applied to address changes in cubicle width, particularly for targets at the same stand-off range, and changes in cubicle depth for targets at different stand-off ranges.

4.3. Limitations and future work

The systematic modelling process employed using Air3D enabled representative and consistent simulation of blast effects. The accuracy of the software has been extensively validated (Rose, 2001) in academic studies. However, the software is, to some extent, inherently limited by its representation of blast phenomenology based on the simplifying assumptions that make it computationally feasible. Similarly, computational limitations on cell size may have introduced some discretisation issues, particularly with regards to the precise positioning of free-field gauges as shown in Figure 10.

Further work to verify the accuracy of these predictions should include experimental blast testing, initially with free-field incident pressure gauges at the recommended separation distances for different stand-off ranges. To extend this, an examination of the reflected pressure and impulse on full-scale test cubicles at recommended separations could be employed.

5. Conclusions

In arena blast tests, a lack of careful consideration of the positioning of target cubicles around a charge can result in either: sparsely distributed targets, which poorly utilise test range space; or, targets positioned too closely together, which can result in undesirable interference effects either increasing or decreasing incident blast wave parameters, depending on the location of the monitoring point.

An extensive and systematic modelling study was undertaken using Air3D to identify the differences in peak incident overpressure and incident positive phase impulse caused by a fixed target obstruction. The study indicated that, in all conditions, a greater separation distance was required to achieve free-field impulse values than free-field pressure. A bespoke recommendation table has been presented that can be used by engineers in the field to identify minimum separation distances for targets at different ranges.

The results indicate that the established ‘rules of thumb’ for separation of targets at different ranges (45°) still hold practical relevance, whilst the recommendation for targets at the same range (two cubicle widths) are generally too conservative and not applicable to all test configurations.

6. Acknowledgements

The analysis on which this paper is based was conducted by the Home Office – Centre for Applied Science and Technology (CAST) as part of a programme of research and development funded and directed by the Centre for the Protection of National Infrastructure (CPNI).

The authors would also like to acknowledge the University of Sheffield for the experimental test data provided for validation.

7. References

Ballantyne, G. J., Whittaker, A. S., Dargush, G. F. and Aref, A. J. (2009) 'Air-blast effects on structural shapes of finite width', Journal of Structural Engineering, 136 (2), pp 152–159.

Codina, R., Ambrosini, D. and de Borbón, F. (2013) 'Numerical Study of Confined Explosions in Urban Environments', International Journal of Protective Structures, 4 (4), pp 591–618.

Needham, C. E. (2009) 'Blast loads and propagation around and over a building'. 26th International Symposium on Shock Waves, Volume 2, pp 1359–1364. Springer Berlin Heidelberg.

Qasrawi, Y., Heffernan, P. J. and Fam, A. (2015) 'Numerical Determination of Equivalent Reflected Blast Parameters Acting on Circular Cross Sections', International Journal of Protective Structures, 6 (1), pp 1–22.

Remennikov, A. M. and Rose, T. A. (2005) 'Modelling blast loads on buildings in complex city geometries', Computers and Structures, 83 (27), pp 2197–2205.

Rickman, D. D. and Murrell, D. W. (2007) 'Development of an improved methodology for predicting airblast pressure relief on a directly loaded wall', Journal of Pressure Vessel Technology, 129 (1), pp 195–204.

Rigby, S., Tyas, A., Bennett, T., Fay, S., Clarke, S. and Warren, J. (2014a) 'A numerical investigation of blast loading and clearing on small targets', International Journal of Protective Structures, 5 (3), pp 253–274.

Rigby, S., Tyas, A., Bennett, T., Clarke, S. and Fay, S. (2014b) 'The negative phase of the blast load', International Journal of Protective Structures, 5 (1), pp 1–20.

Rose, T. A. (2001) An approach to the evaluation of blast loads on finite and semi-infinite structures. Doctoral dissertation. UK: Cranfield University.

Rose, T. A. (2006) 'A Computational Tool for Airblast Calculations', *Air3d version 9 users' guide*. UK: Cranfield University.

Shi, Y., Hao, H. and Li, Z. X. (2007) 'Numerical simulation of blast wave interaction with structure columns', Shock Waves, 17 (1–2), pp 113–133.

Smith, P. D. and Rose, T. A. (2000) 'The influence of urban geometry on blast wave resultants', Proceedings of the 16th Military Aspects of Blast and Shock Symposium, vol. 10, p. 15. UK: Oxford.

Tyas, A., Warren, J. A., Bennett, T. and Fay, S. (2011) 'Prediction of clearing effects in far-field blast loading of finite targets', Shock Waves, 21 (2), pp 111–119.